JACS
JOURNAL OF THE AMERICAN CHEMICAL SOCIETY
Article
pubs.acs.org/JACS

Helicene Quinones: Redox-Triggered Chiroptical Switching and Chiral Recognition of the Semiquinone Radical Anion Lithium Salt by Electron Nuclear Double Resonance Spectroscopy

David Schweinfurth,[†] Michal Zalibera,[‡] Michael Kathan,[†] Chengshuo Shen,[§] Marcella Mazzolini,[†] Nils Trapp,[†] Jeanne Crassous,[§] Georg Gescheidt,*[,‡] and François Diederich*[,†]

[†]Laboratory of Organic Chemistry, ETH Zurich, Vladimir-Prelog-Weg 3, CH-8093 Zurich, Switzerland

[‡]Institute of Physical and Theoretical Chemistry, Graz University of Technology, Stremayrgasse 9, A-8010 Graz, Austria

[§]Institut des Sciences Chimiques de Rennes, UMR 6226, CNRS—Université de Rennes 1, Campus de Beaulieu, 35042 Rennes Cedex, France

Supporting Information

ABSTRACT: We present the synthesis and characterization of enantiomerically pure [6]helicene *o*-quinones (*P*)-(+)-**1** and (*M*)-(−)-**1** and their application to chiroptical switching and chiral recognition. (*P*)-(+)-**1** and (*M*)-(−)-**1** each show a reversible one-electron reduction process in their cyclic voltammogram, which leads to the formation of the semiquinone radical anions (*P*)-(+)-**1**$^{\bullet-}$ and (*M*)-(−)-**1**$^{\bullet-}$, respectively. Spectroelectrochemical ECD measurements give evidence of the reversible switching between the two redox states, which is associated with large differences of the Cotton effects [$\Delta(\Delta\varepsilon)$] in the UV and visible regions. The reduction of (±)-**1** by lithium metal provides [Li$^+${(±)-**1**$^{\bullet-}$}], which was studied by EPR and ENDOR spectroscopy to reveal substantial delocalization of the spin density over the helicene backbone. DFT calculations demonstrate that the lithium hyperfine coupling $A(^7\mathrm{Li})$ in [Li$^+${(±)-**1**$^{\bullet-}$}] is very sensitive to the position of the lithium cation. On the basis of this observation, chiral recognition by ENDOR spectroscopy was achieved by complexation of [Li$^+${(*P*)-(+)-**1**$^{\bullet-}$}] and [Li$^+${(*M*)-(−)-**1**$^{\bullet-}$}] with an enantiomerically pure phosphine oxide ligand.

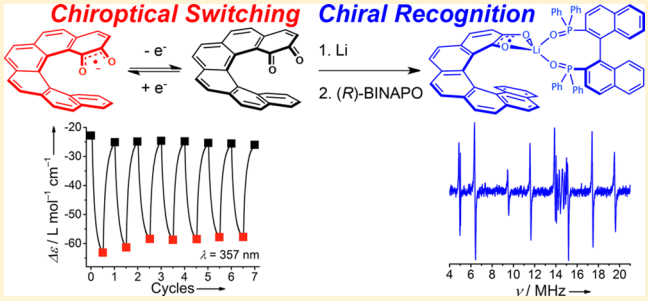

INTRODUCTION

Molecular switches allow control of the change from one state to another by external stimuli on the nanoscale.[1] Chiroptical switching materials are especially attractive, since they might find application in the areas of data storage, optical displays, and light modulators.[2] Helicenes[3] are ideal building blocks for switches with a large chiroptical response because they exhibit very large optical rotation values and strong Cotton effects in their electronic circular dichroism (ECD) spectra.[4]

The chiroptical properties of [*n*]helicenes can be controlled not only by the number of fused rings *n*[4] but also by complexation with appropriate metal ions.[5] Furthermore, the stilbenoid bridging of two [6]helicenes by a conjugated ethene-1,2-diyl unit leads to a very large, amplified increase of the chiroptical properties, as recently reported by our group.[6] After reduction to the nonconjugated ethane-1,2-diyl linker, the system behaved similarly to two independent [6]helicenes. In contrast to this irreversible reduction process, some of us recently reported the reversible chiroptical switching in an electroactive ruthenium−vinylhelicene complex.[7] Despite their potential application in organic electronics,[2] only a very limited number of additional examples of electrochemically triggered, helicene-based chiroptical switches have been reported to date, comprising a tetrathiafulvalene−[6]helicene conjugate,[8] a thiophene-based [7]helicene,[9] and an enantiopure "helquat" system.[10]

Further improved chiroptical switches are desired that feature a higher difference $\Delta(\Delta\varepsilon)$ in the ECD spectra of their different states. Their bistable states, accessed by reversible switching, should also show distinctly different bands in various regions of the ECD spectrum. To work toward these goals, we decided to exploit the well-known electrochemical switching behavior of quinones.[11] Whereas helicene bis-*p*-quinones were studied in great detail by Katz and co-workers with respect to mixed valency[12] and supramolecular aggregation,[13] the synthesis and properties of plain helicene *o*-quinones[14] remain unexplored. *o*-Quinones are highly attractive not only because they can be reduced to the catecholate dianion via the semiquinone radical anion but also because they bind metal ions[15] and undergo a range of chemical transformations,[16] which allows for fine-tuning of their properties.

Helicenes are known for their photophysical properties,[4,17] but they were also studied in diverse fields, such as asymmetric

Received: July 11, 2014
Published: August 25, 2014

 © 2014 American Chemical Society dx.doi.org/10.1021/ja5069323 | J. Am. Chem. Soc. 2014, 136, 13045−13052

catalysis,[18] chiral recognition,[19] and surface science.[13b,20] Therefore, it can be expected that an elaborately designed helicene-based chiroptical switch will also find application in areas such as chiral recognition. In the latter field, the formation of diastereoisomers between a chiral host and a chiral guest has been studied extensively by numerous spectroscopic techniques.[21] Nonetheless, reports of chiral recognition of organic radicals by EPR and electron nuclear double resonance (ENDOR) spectroscopy are extremely rare.[22]

Here, we present a comprehensive study on the synthesis and properties of the new enantiomerically pure [6]helicene *o*-quinones (*P*)-(+)-**1** and (*M*)-(−)-**1** (Figure 1). The reversible

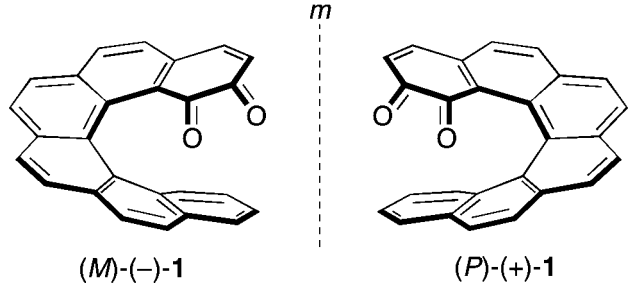

Figure 1. Molecular structures of [6]helicene *o*-quinones (*M*)-(−)-**1** and (*P*)-(+)-**1**.

reduction of **1** to the semiquinone radical anion $\mathbf{1}^{\bullet-}$ was exploited for chiroptical switching in the UV and visible regions. Furthermore, detailed EPR and ENDOR spectroscopic investigations of the lithium radical salt of $\mathbf{1}^{\bullet-}$, combined with high-level DFT calculations, paved the way for chiral recognition of the radical anion lithium salt with the help of an enantiopure phosphine oxide chelator.

RESULTS AND DISCUSSION

Synthesis and Crystal Structures. Transition-metal-catalyzed [2 + 2 + 2] cyclotrimerization[23] was used as the key step to assemble the helical backbone[24] in the synthesis of (*P*)-(+)-**1** and (*M*)-(−)-**1** (Scheme 1 and section 2SI in the

Scheme 1. Key Steps in the Synthesis of (*P*)-(+)-1 and (*M*)-(−)-1[a]

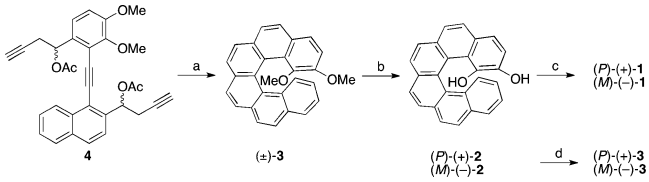

[a](a) (1) [Ni(COD)$_2$], PPh_3, THF, 22 °C, 12 h; (2) TsOH·H_2O, toluene, 80 °C, 3 h, 46% over two steps. (b) (1) BBr_3, CH_2Cl_2, −78 °C, 3 h, 70%; (2) enantioseparation by HPLC on a chiral stationary phase. (c) AgO, CH_3CN, 22 °C, 1 h, 99% and 99%. (d) CH_3I, K_2CO_3, acetone, 50 °C, 8 h, 68% and 52%. COD = 1,5-cyclooctadiene. TsOH = *p*-toluenesulfonic acid.

Supporting Information). The racemic helicene catechol (±)-**2** could be obtained by cleavage of the methoxy groups of (±)-**3** employing BBr_3 in CH_2Cl_2. Separation of enantiomers by preparative HPLC on a chiral stationary phase [covalent (*S*,*S*)-Whelk-O 1, see section 2SI] provided (*P*)-(+)-**2** and (*M*)-(−)-**2** in enantiopure form, which were oxidized in quantitative yields using AgO in CH_3CN to provide the target compounds. Methylation of (*P*)-(+)-**2** and (*M*)-(−)-**2** was used to obtain (*P*)-(+)-**3** and (*M*)-(−)-**3**, respectively, in enantiopure form.

Helicene catechol (±)-**2** is air-sensitive in solution and undergoes uncontrolled oxidation reactions, which lead to a complex mixture of products. Nevertheless, it was possible to grow single crystals suitable for X-ray diffraction analysis by slow diffusion of *n*-hexane into a chloroform solution at −30 °C under a nitrogen atmosphere. In contrast, (±)-**1** is stable under ambient conditions and could also be crystallized by slow diffusion of *n*-hexane into a chloroform solution at −30 °C. Whereas (±)-**2** crystallizes in the orthorhombic space group *Pbca*, (±)-**1** crystallizes in the monoclinic space group $P2_1/c$ (see Figure 2 and section 3SI).

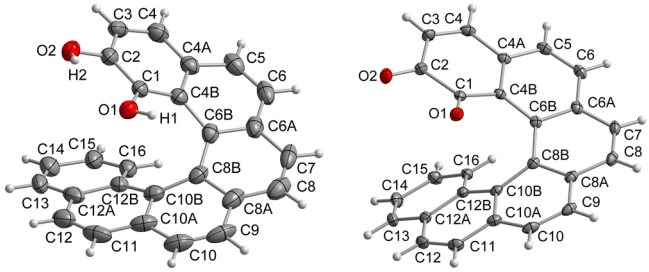

Figure 2. X-ray structures of (±)-**2** (left) and (±)-**1** (right). Only the (*P*)-(+) enantiomers are shown. Solvent molecules were omitted for clarity, and the ellipsoids were drawn at 50% probability. *T* = 100 K.

As expected, the oxidation of (±)-**2** to (±)-**1** is reflected by bond length differences in the two molecular structures.[25] Before the oxidation, the bond lengths C(1)−O(1) and C(2)−O(2) amount to 1.346(4) and 1.362(4) Å, respectively; after oxidation to the quinone, these bonds are considerably shortened [1.210(2) and 1.211(2) Å, respectively]. Whereas the C(1)−C(2) distance of 1.394(5) Å is proof of the aromatic character in **2**, the value of 1.557(2) Å for the same bond in **1** is indicative of a single bond, which is in agreement with the quinoidal structure. Compound (±)-**1** is also characterized by an unexpectedly large torsion angle O(1)−C(1)−C(2)−O(2) of −18.7(2)°, compared to a value of −4.1(4)° in (±)-**2**. Structural parameters that describe the pitch heights and pitch angles in (±)-**1** and (±)-**2** can be found in Table 2SI.

Electrochemistry, Chiroptical Switching, and TD-DFT Calculations. Cyclic voltammetry (CV) was used to study the reduction behavior of (±)-**1** in acetonitrile. The first reversible reduction was observed at $E_{1/2}$ = −1.00 V (vs $Fc^{+/0}$, ΔE_p = 0.07 V), whereas the second reduction process was irreversible with E_{pc} = −1.71 V (see Figure 3SI). This points to the formation of a stable semiquinone radical anion (±)-$\mathbf{1}^{\bullet-}$ as the first reduction product. Further reduction to the catecholate dianion is irreversible possibly because of the protonation of this very basic species. Under similar conditions, the prototypical 3,5-di-*tert*-butyl-*o*-benzoquinone showed a reversible first reduction at −0.92 V vs $Fc^{+/0}$ in acetonitrile.[26]

The marked difference between light yellow **2** and dark red **1** is visible to the naked eye. To gain further insight into the electronic structures of the two compounds, UV/vis and ECD spectroscopy in acetonitrile was measured (Table 1, Table 3SI, and Figure 4SI). Because the CV results point to the formation of a stable semiquinone radical anion after reduction, spectroelectrochemical measurements with an optically transparent thin layer electrochemical (OTTLE) cell[27] were used to study the UV/vis and ECD spectra of $\mathbf{1}^{\bullet-}$.

dx.doi.org/10.1021/ja5069323 | J. Am. Chem. Soc. 2014, 136, 13045−13052

Table 1. UV/Visible and ECD Spectra Recorded in Acetonitrile[a]

compd	λ, nm (ε, L mol^{-1} cm^{-1})	λ, nm ($\Delta\varepsilon$, L mol^{-1} cm^{-1})
(*P*)-(+)-**1**	243 (54100), 266 (27100), 291 (25000), 307 sh[b] (21200), 329 sh (12000), 388 (3500), 471 bsh[c] (1600)	243 (−49), 276 (−72), 307 sh (+27), 329 (+101), 367 (+20), 387 (+25), 471 (+12)
(*P*)-(+)-**1**$^{\bullet-}$	245 (44000), 280 (32500), 299 sh (22700), 348 sh (11000), 447 br. (3700), 625 br. (1900)	277 (−73), 318 sh (+32), 348 (+69), 385 (+31), 505 (+15), 628 (+5)
(*P*)-(+)-**2**	243 (43300), 271 (25500), 307 sh (14900), 320 (17800), 351 sh (9100), 380 sh (3200), 400 (1500), 426 (1200)	245 (−122), 272 (−69), 331 (+122), 370 sh (+33)
(*P*)-(+)-**3**	244 (42600), 258 (41700), 307 sh (16800), 319 (23000), 330 sh (19500), 352 sh (11300), 398 (1300), 421 (1200)	247 (−142), 271 sh (−63), 330 (+159), 357 sh (+64)
(*P*)-(+)-[6]helicene[d]	246 (51700), 324 (28300)	246 (−272), 324 (+259)

[a]Only the spectral characterization for the (*P*)-(+) enantiomers is listed [see Table 3SI for ECD spectral data of the (*M*)-(−) enantiomers]. Monoreduced (*P*)-(+)-**1**$^{\bullet-}$ was investigated by UV/vis and ECD spectroelectrochemistry in an OTTLE cell (0.1 M NBu_4PF_6 was used as an electrolyte). Solutions of (*P*)-(+)-**2** are very air-sensitive and were prepared in a glovebox under exclusion of oxygen and water. [b]Shoulder. [c]Broad shoulder. [d]Only major transitions are given.[4]

The bisignate shape of the ECD spectra of helicenes allows for the assignment of (*P*)- and (*M*)-enantiomers. Accordingly, the ECD spectra of the fully aromatic (*P*)-(+)-**2** and (*P*)-(+)-**3** show the typical ^1B_a band in the narrow range 245−247 nm with negative sign and a less intense band around 271 nm (Table 1). In contrast, the quinoidal (*P*)-(+)-**1** displays only a weak band at 243 nm but a major transition at 276 nm with negative sign. However, all three compounds show the typical ^1B_b band in the close range 329−331 nm with positive sign. The spectra of (*P*)-(+)-**2** and (*P*)-(+)-**3** also compare remarkably well with the spectrum of pristine (*P*)-(+)-[6]-helicene, which shows ^1B_a and ^1B_b bands at 246 and 324 nm, respectively.[4] Even though the position of the major transitions seems to be unaltered by the substitution pattern, the intensities of the Cotton effects are significantly influenced. Whereas (*P*)-(+)-[6]helicene shows a Cotton effect of +259 L mol^{-1} cm^{-1} at the ^1B_b band (324 nm), this value decreases from (*P*)-(+)-**3** to (*P*)-(+)-**2** to a value of +122 L mol^{-1} cm^{-1} in the latter (Table 1). In accordance with our findings, it was recently pointed out that substitution of [6]helicenes in the 1- and 2-position drastically decreases the Cotton effect because of steric reasons.[17d]

Nonetheless, compared to unsubstituted (*P*)-(+)-[6]-helicene, a completely new band appears at 471 nm in the visible region of the ECD spectrum of (*P*)-(+)-**1**, causing the red color. Upon reduction, the ^1B_b band in (*P*)-(+)-**1**$^{\bullet-}$ is shifted to 348 nm, and two bands in the visible region appear at 505 and 628 nm. The differences in the ECD spectra of the quinone and semiquinone radical anions were exploited for chiroptical switching (Figure 3). (*M*)-(−)-**1** could be reversibly reduced and reoxidized over several cycles. Large spectral differences $\Delta(\Delta\varepsilon)$ of up to 40 L mol^{-1} cm^{-1} were found at 357 nm, whereas smaller differences $\Delta(\Delta\varepsilon)$ were found at 635 nm accounting to 4 L mol^{-1} cm^{-1}. However, the latter change is significant because it can be ascribed to the appearance of a new band, which corresponds to an on−off chiroptical switching. The switching performance of this purely organic carbohelicene is comparable to the known metalorganic diruthenium−vinylhelicene system, in which switching was reported at 340 and 500 nm.[7]

TD-DFT calculations with the Gaussian 09 software package[28] were carried out to uncover the chiroptical properties of (*P*)-(+)-**2**, (*P*)-(+)-**1**, and (*P*)-(+)-**1**$^{\bullet-}$. A geometry optimization at the ωB97X-D/6-31g(d,p) level of theory afforded molecular geometries that compare well with the X-ray crystal structures. The calculated ECD spectrum [CAM-B3LYP/6-31g(d,p)] of (*P*)-(+)-**2** agrees well with the

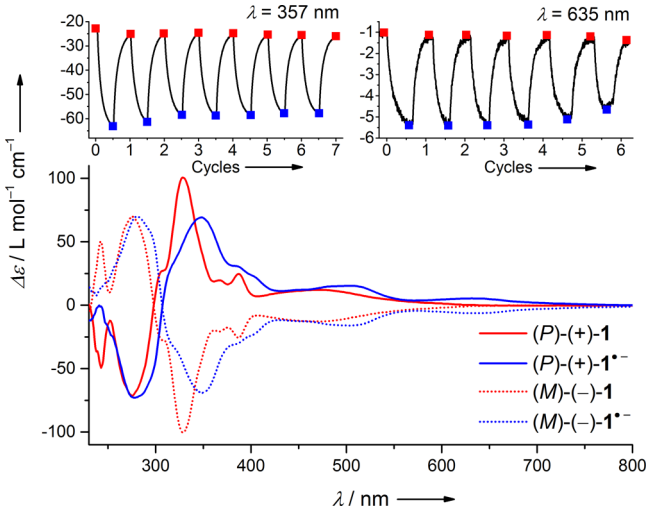

Figure 3. ECD spectra and chiroptical switching in acetonitrile. Spectra of (*P*)-(+)-**1**$^{\bullet-}$ and (*M*)-(−)-**1**$^{\bullet-}$ were generated electrochemically in an OTTLE cell. Reversible electrochemical switching for several cycles is shown for the (*M*)-(−) enantiomer at two different wavelengths (top).

experimental data, reproducing the bisignated shape (Figure 8SI). Whereas the lowest-energy band around 400 nm corresponds to the HOMO → LUMO transition, the band around 330 nm (^1B_b band) has major contributions from HOMO − 1 → LUMO and HOMO → LUMO + 1. These results compare well with the electronic structure of (*P*)-(+)-[6]helicene.[4]

In comparison, the HOMO−LUMO gap in (*P*)-(+)-**1** is slightly decreased. Thus, the HOMO → LUMO transition is bathochromically shifted to 471 nm (Figure 4), in agreement with the red color in the solid state and in solution. In contrast, the transition corresponding to the ^1B_b band cannot be assigned unambiguously to distinct electronic levels, but it is a mixture of several contributing transitions. The HOMO and the LUMO are very well spatially separated in (*P*)-(+)-**1** (Figure 4). Whereas the LUMO is concentrated on the electron-poor six-membered quinone ring, the HOMO is delocalized over the electron-rich helicene backbone. The HOMO−LUMO transition therefore has a significant charge-transfer character.

The low-energy bands in the ECD spectra of (*P*)-(+)-**1**$^{\bullet-}$ are due to the open-shell character of this species. Accordingly, the band around 630 nm can be explained by an α-SOMO → α-SOMO + 1 transition, whereas the band around 510 nm is

dx.doi.org/10.1021/ja5069323 | J. Am. Chem. Soc. 2014, 136, 13045−13052

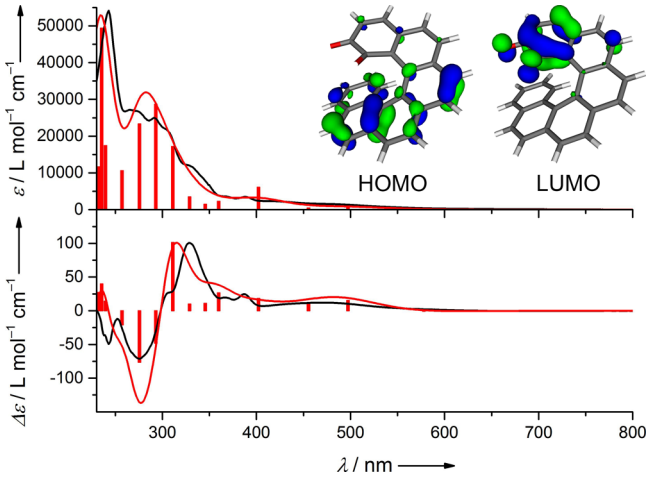

Figure 4. TD-DFT calculations [CAM-B3LYP/6-31g(d,p)] on (*P*)-(+)-**1** in acetonitrile. Calculated (red) and experimental (black) UV/vis (top) and ECD (bottom) spectra are shown. Red bars indicate major transitions calculated. In the inset, the calculated frontier orbitals are shown.

characterized by an α-SOMO → α-SOMO + 2 transition (Figure 9SI). The transition around 350 nm, which corresponds to the ^1B_b band, has major contributions from the α-SOMO − 2 → α-SOMO + 1 transition.

EPR and ENDOR Spectroscopy. Because the generation of the semiquinone radical anion is crucial for chiroptical switching, we used temperature-dependent EPR and ENDOR techniques to gain more insight into the electronic structure of the radical species.[29] Elemental lithium in THF was used as the reducing agent to form [Li$^+${(±)-**1**$^{\bullet-}$}], which was stable under exclusion of water and air. Well-resolved X-band EPR spectra of [Li$^+${(±)-**1**$^{\bullet-}$}] (Figure 5 and Figure 5SI) could be recorded at variable temperatures down to 165 K (Table 4SI). A signal was detected at g = 2.0043, which is close to that of the free electron

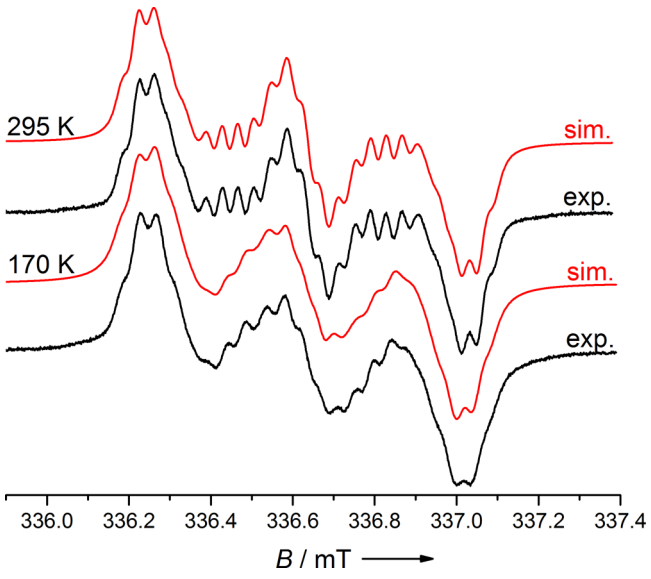

Figure 5. X-band (9.4506 GHz) EPR spectra (black) of [Li$^+${(±)-**1**$^{\bullet-}$}] in THF at 295 K (top) and 170 K (bottom) with simulations (red). Natural abundances of 7.5% for ^{6}Li (S = 1) and 92.5% for ^{7}Li (S = 3/2) and corresponding g_n ratio were taken into account for EPR simulations.[32]

(g_e = 2.0023) and thus indicative of an organic radical. Simulations of the spectra revealed hyperfine couplings with a total of seven protons in the range −10.20 to −0.30 MHz. This points to the delocalization of the radical over a large part of the conjugated helicene. Furthermore, hyperfine coupling (hfc) with lithium had also to be taken into account for a well-fitting simulation, which hints at the formation of a rather tight ion pair in solution.[30] The hfc constant with lithium increased from −1.57 MHz at 295 K to −1.40 MHz at 165 K, whereas the proton couplings were virtually not affected.

To prove the formation of an ion pair in solution, variable-temperature ENDOR spectroscopy was carried out in the range 250−165 K (Table 4SI).[31] The formation of [Li$^+${(±)-**1**$^{\bullet-}$}] could be unequivocally established because the ENDOR resonances related to the hfc with lithium are well distinguishable in the low-frequency region of the ENDOR spectrum. In contrast, the multiple proton hfcs were resolved at the high-frequency region because of the different Larmor frequencies of the two nuclei.[32] The hfcs obtained from the ENDOR spectra match the simulated EPR data very well (Table 4SI). Nevertheless, the simulation of EPR data is crucial for determining the exact number of small proton couplings. Furthermore, general electron−nuclear−nuclear triple resonance (TRIPLE) spectroscopy at 165 K was used to determine the relative sign of the hfc constants (Figure 6SI).

In comparison to the ENDOR spectrum of the prototypical complex [Li(3,5-di-*tert*-butyl-*o*-benzosemiquinone)] in THF at 190 K [A(^{7}Li) = −1.75 MHz],[31] the value obtained for [Li$^+${(±)-**1**$^{\bullet-}$}] in THF at 180 K is slightly higher [A(^{7}Li) = −1.45 MHz]. To understand the parameters affecting the lithium hfc in more detail and to assign the proton hfcs, DFT calculations were carried out. A geometry optimization and calculations of the isotropic Fermi contact couplings of [Li$^+${(±)-**1**$^{\bullet-}$}] were achieved at the uωB97X-D/6-31g(d,p) level of theory. The resulting spin density map (Table 2) shows the delocalization of the unpaired electron over the whole helicene structure. Furthermore, the calculation of the Fermi contact interactions allowed for the assignment of hfcs determined by EPR and ENDOR spectroscopy (Table 2) to the individual nuclei. The calculated values are in very good agreement with the experimental hfc constants, and the largest proton couplings can unambiguously be assigned to the hydrogen atoms H4 and H6.

The lithium coupling is calculated with a value of −1.26 MHz, which is slightly higher than the measured values of −1.57 MHz (295 K) and −1.40 MHz (165 K). Recently, two models were proposed to explain the temperature dependence of the sodium hyperfine coupling in a related corannulene-based semiquinone radical anion.[26] By use of these models, the temperature dependence of the lithium hyperfine coupling in [Li$^+${(±)-**1**$^{\bullet-}$}] can be explained by a movement of the lithium atom.

In the first model, the lithium atom is moved along an axis toward the semiquinone radical anion, in the O═C−C═O plane, which decreases the value of A(^{7}Li) toward the negative, whereas A(^{7}Li) nears zero when the lithium atom is moved away from the semiquinone radical anion (Figure 10SI). In the second model, the Li−O distances are kept constant, and the lithium atom is moved on a circle around the semiquinone radical anion. In this model, a maximum value of A(^{7}Li) is reached at around 10° (Figure 11SI).

Even though both models are able to explain the temperature dependence of A(Li) by the displacement of the lithium atom,

dx.doi.org/10.1021/ja5069323 | J. Am. Chem. Soc. 2014, 136, 13045−13052

Table 2. Hyperfine Coupling Constants from Simulations of X-Band (9.4506 GHz) EPR Spectra of [Li$^+${(±)-1$^{\bullet-}$}] in THF and Calculated Values [uωB97X-D/6-31g(d,p)][a]

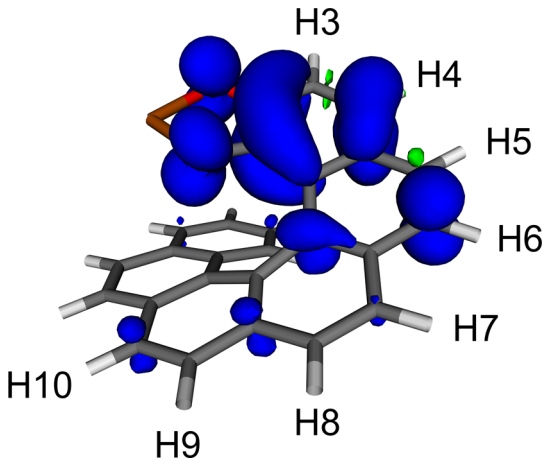

		A, MHz							
method	T, K	^{7}Li	H4	H5	H6	H7	H8	H9	H10
EPR	295	−1.57	−10.19	±1.23	−5.84	±1.03	−0.73	+0.33	±1.14
EPR	165	−1.40	−10.01	±1.27	−5.83	±1.06	−0.72	+0.29	±1.21
ENDOR	165	−1.39	−10.00	±1.24	−5.85	±1.04	−0.72	+0.32	
DFT		−1.26	−10.98	+1.97	−5.43	−1.04	+0.71	+0.62	−1.14

[a]Natural abundances of 7.5% for ^{6}Li (S = 1) and 92.5% for ^{7}Li (S = 3/2) and corresponding g_n ratio were taken into account for EPR simulations.[32] Relative signs of hyperfine coupling constants were determined by general TRIPLE (Figure 6SI) spectroscopy (± marks ambiguous assignment), whereas the atom assignment is based on DFT results. Hyperfine coupling with H3 and H11−H16 is negligible according to DFT. Above the table, the spin density distribution in (*P*)-(+)-**1**$^{\bullet-}$ predicted by DFT calculations [uωB97X-D/6-31g(d,p)] is shown.

they suffer from a major drawback: They do not take the coordination environment of the lithium atom into account. Because it is well-known that lithium cations prefer a tetrahedral coordination sphere,[33] it is most likely that the coordination environment of the lithium atom in [Li$^+${(±)-**1**$^{\bullet-}$}] is completed by THF molecules. Nevertheless, both models show that the lithium hfc in [Li$^+${(±)-**1**$^{\bullet-}$}] is very sensitive even toward minor structural changes. For example, a displacement of the lithium atom by only 2.5° leads to a change of A(^{7}Li) from hfc −1.26 MHz in the optimized structure to −1.40 MHz (Figure 11SI), a difference that could be easily determined by ENDOR spectroscopy.

Chiral Recognition by ENDOR Spectroscopy. Led by the premise that the lithium cation in [Li$^+${(±)-**1**$^{\bullet-}$}] is coordinated by two THF molecules and that the lithium hfc is very sensitive toward structural changes, chiral recognition in diastereoisomeric complexes should be possible. Displacing the coordinating THF molecules in enantiopure [Li$^+${(*P*)-(+)-**1**$^{\bullet-}$}] and [Li$^+${(*M*)-(−)-**1**$^{\bullet-}$}] by homochiral ligands should lead to diastereoisomeric complexes with a different lithium coordination and hence different A(^{7}Li) values mirroring the changed molecular environment.

To test this hypothesis, a range of chiral ligands (Scheme 2SI) featuring bis(methoxy ether) or bisoxazoline coordination motifs were added to [Li$^+${(±)-**1**$^{\bullet-}$}] in THF. Unfortunately, the ENDOR spectra remained completely unaltered, indicating that the coordination failed. To compete effectively with the coordinated THF molecules, stronger lithium-binding chelators are crucial. Because Ph_3PO is known to bind strongly to lithium,[34] we turned our attention to (*R*)-(+)-2,2′-bis(diphenylphosphanyl)-1,1′-binaphthyldioxide [(*R*)-(+)-BINAPO], which was recently used as a chiral organocatalyst.[35] Addition of (*R*)-(+)-BINAPO to [Li$^+${(±)-**1**$^{\bullet-}$}] in THF affected the whole ENDOR spectrum (Figure 7SI). Whereas the total number of hyperfine splittings remained constant, the small, but significant, changes of the lithium and proton hfcs (Table 5SI) indicate the formation of [{(*R*)-(+)-BINAPO}Li$^+${(±)-**1**$^{\bullet-}$}]. Subsequently, the diastereoisomers [{(*R*)-(+)-BINAPO}Li$^+${(*P*)-(+)-**1**$^{\bullet-}$}] and [{(*R*)-(+)-BINAPO}Li$^+${(*M*)-(−)-**1**$^{\bullet-}$}] were prepared, and their ENDOR spectra were recorded. The diastereoisomers can be distiguished by their lithium hfc with a temperature optimum at 210 K (Table 5SI). Whereas [{(*R*)-(+)-BINAPO}Li$^+${(*P*)-(+)-**1**$^{\bullet-}$}] shows an A(^{7}Li) value of −1.76 MHz at 210 K, a value of −1.62 MHz was found for [{(*R*)-(+)-BINAPO}-Li$^+${(*M*)-(−)-**1**$^{\bullet-}$}] (Figure 6). The spectrum of the racemate [{(*R*)-(+)-BINAPO}Li$^+${(±)-**1**$^{\bullet-}$}] gives the average value of −1.69 MHz. Moreover, the two diasteroisomers (Table 5SI) have distinct hfcs with H4.

Besides early reports on chiral recognition of organic radicals by ENDOR spectroscopy,[22] paramagnetic transition-metal complexes of vanadium[36] and copper[37] were recently used for chiral recognition of small molecules in frozen solution at low temperatures. In comparison, this is the first report in which lithium is used not only as the reducing agent but also as a probe for chirality. Remarkably, the very sensitive lithium hfc monitors the recognition process in liquid solution, under reaction conditions including dynamic phenomena and at which chiral recognition takes place.

In comparison to NMR methods, the much higher sensitivity of the ENDOR experiment allows the study of very low concentrated samples.[32] Furthermore, the hfcs can be determined to about 10^{-3}% accuracy,[32] which permits reliable chiral discrimination. Our study also helps to understand the role of chiral phosphine oxides as organocatalysts in enantioselective reactions.[35]

dx.doi.org/10.1021/ja5069323 | J. Am. Chem. Soc. 2014, 136, 13045−13052

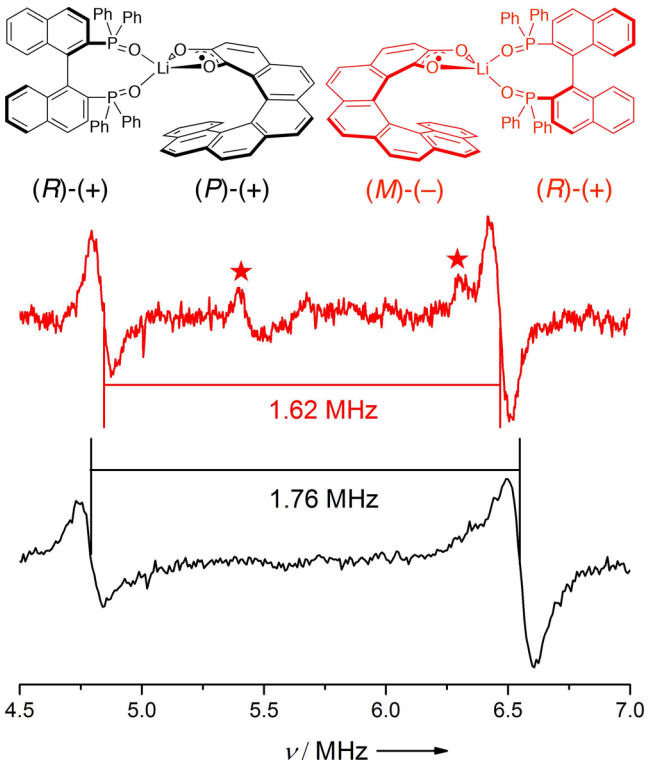

Figure 6. ENDOR spectra of [{(*R*)-(+)-BINAPO}Li$^+${(*P*)-(+)-**1**$^{\bullet-}$}] (black) and [{(*R*)-(+)-BINAPO}Li$^+${(*M*)-(−)-**1**$^{\bullet-}$}] (red) in THF at 210 K. Only the low-frequency region is shown. Asterisks show artifacts arising from strong RF irradiation.

SUMMARY AND CONCLUSIONS

We have presented the synthesis and characterization of the enantiomerically pure [6]helicene *o*-quinones (*P*)-(+)-**1** and (*M*)-(−)-**1**. Their reversible one-electron reduction to the semiquinone radical anions (*P*)-(+)-**1**$^{\bullet-}$ and (*M*)-(−)-**1**$^{\bullet-}$ was exploited for chiroptical switching. UV/vis and ECD spectroelectrochemistry were used to study the electrochromic behavior. Reversible switching over several cycles between the two states was associated with differences $\Delta(\Delta\varepsilon)$ of the Cotton effect in the UV and in the visible regions of the ECD spectrum. The switching performance of this purely organic helicene is comparable to a known metalorganic diruthenium–vinylhelicene system.[7] TD-DFT calculation could prove that the incorporation of a quinoidal unit into a helicene affects its chiroptical properties, as transitions associated with the quinoidal part appear in the ECD spectrum. The incorporation of other well-known electrochromic units, such as transition-metal polypyridyl complexes,[38] into the π system of helicenes might therefore lead to novel chiroptical switches.

EPR and ENDOR spectroscopy on [Li$^+${(±)-**1**$^{\bullet-}$}], which was generated by reduction with lithium metal, showed delocalization of the spin density over a large part of the helicene. DFT calculations were used for the atom assignment of the observed hfcs. The high sensitivity of the $A(^7\mathrm{Li})$ was used for the chiral recognition of the diastereomeric complexes [{(*R*)-(+)-BINAPO}Li$^+${(*P*)-(+)-**1**$^{\bullet-}$}] and [{(*R*)-(+)-BINAPO}Li$^+${(*M*)-(−)-**1**$^{\bullet-}$}] by ENDOR spectroscopy. Considering the variety of radical anions known,[39] this methodology might be of general interest. It also has the potential to obtain insight into specific interactions of chiral phosphine oxides, which are currently used as organocatalysts in enantioselective reactions.[35] Finally, the potential of phosphoric acids[40] based on the enantiopure helicenediols (*M*)-(−)-**2** and (*P*)-(+)-**2** in asymmetric organocatalysis is under investigation.

ASSOCIATED CONTENT

Supporting Information

Synthesis and full characterization of new compounds, X-ray crystallographic data, details of EPR and ENDOR spectroscopy, notes on DFT calculations, and crystallographic data in CIF format. This material is available free of charge via the Internet at http://pubs.acs.org.

AUTHOR INFORMATION

Corresponding Authors

diederich@org.chem.ethz.ch

Notes

The authors declare no competing financial interest.

ACKNOWLEDGMENTS

This work was supported by a grant from the Swiss National Science Foundation (SNF). D.S. acknowledges the DAAD for a postdoctoral fellowship. M.Z. acknowledges financial support from the Stiftung ProBono and the TU and NAWI Graz. J.C. thanks the Ministère de l'Education Nationale, de la Recherche et de la Technologie, the Centre National de la Recherche Scientifique (CNRS), and the ANR (12-BS07-0004-METAL-HEL-01) for financial support. We thank Dr. Bruno Bernet for the help with interpretation of NMR spectra, and Oliver Dumele and Dr. Jesse Roose for helpful discussions. Fritz Weißer is acknowledged for proofreading the manuscript.

REFERENCES

(1) *Molecular Switches*, 2nd ed.; Feringa, B. L., Browne, W. R., Eds.; Wiley-VCH: Weinheim, Germany, 2011; Vols. *1* and *2*.
(2) (a) Canary, J. W. *Chem. Soc. Rev.* **2009**, *38*, 747–756. (b) Zhang, G.; Zhang, D.; Zhu, D. In *Electrochemistry of Functional Supramolecular Systems*; Ceroni, P., Credi, A., Venturi, M., Eds.; John Wiley & Sons: Hoboken, NJ, 2010; pp 447–476. (c) Browne, W. R.; Feringa, B. L. In *Molecular Switches*, 2nd ed.; Feringa, B. L., Browne, W. R., Eds.; Wiley-VCH: Weinheim, Germany, 2011; Vol. *1*, pp 121–179.
(3) (a) Shen, Y.; Chen, C.-F. *Chem. Rev.* **2012**, *112*, 1463–1535. (b) Gingras, M. *Chem. Soc. Rev.* **2013**, *42*, 968–1006. (c) Gingras, M.; Félix, G.; Peresutti, R. *Chem. Soc. Rev.* **2013**, *42*, 1007–1050. (d) Gingras, M. *Chem. Soc. Rev.* **2013**, *42*, 1051–1095.
(4) Nakai, Y.; Mori, T.; Inoue, Y. *J. Phys. Chem. A* **2012**, *116*, 7372–7385.
(5) (a) Gilbert, A. M.; Katz, T. J.; Geiger, W. E.; Robben, M. P.; Rheingold, A. L. *J. Am. Chem. Soc.* **1993**, *115*, 3199–3211. (b) Dai, Y.; Katz, T. J. *J. Org. Chem.* **1997**, *62*, 1274–1285. (c) Graule, S.; Rudolph, M.; Vanthuyne, N.; Autschbach, J.; Roussel, C.; Crassous, J.; Réau, R. *J. Am. Chem. Soc.* **2009**, *131*, 3183–3185. (d) Norel, L.; Rudolph, M.; Vanthuyne, N.; Williams, J. A. G.; Lescop, C.; Roussel, C.; Autschbach, J.; Crassous, J.; Réau, R. *Angew. Chem., Int. Ed.* **2010**, *49*, 99–102. (e) Anger, E.; Rudolph, M.; Shen, C.; Vanthuyne, N.; Toupet, L.; Roussel, C.; Autschbach, J.; Crassous, J.; Réau, R. *J. Am. Chem. Soc.* **2011**, *133*, 3800–3803. (f) Shen, C.; Anger, E.; Srebro, M.; Vanthuyne, N.; Deol, K. K.; Jefferson, T. D.; Muller, G.; Williams, J. A. G.; Toupet, L.; Roussel, C.; Autschbach, J.; Réau, R.; Crassous, J. *Chem. Sci.* **2014**, *5*, 1915–1927. (g) Mendola, D.; Saleh, N.; Vanthuyne, N.; Roussel, C.; Toupet, L.; Castiglione, F.; Caronna, T.; Mele, A.; Crassous, J. *Angew. Chem., Int. Ed.* **2014**, *53*, 5786–5790. (h) Anger, E.; Srebro, M.; Vanthuyne, N.; Roussel, C.; Toupet, L.; Autschbach, J.; Réau, R.; Crassous, J. *Chem. Commun.* **2014**, *50*, 2854–

2856. (i) For a review see the following: Saleh, N.; Shen, C.; Crassous, J. *Chem. Sci.* **2014**, *5*, 3680−3694.
(6) Roose, J.; Achermann, S.; Dumele, O.; Diederich, F. *Eur. J. Org. Chem.* **2013**, 3223−3231.
(7) Anger, E.; Srebro, M.; Vanthuyne, N.; Toupet, L.; Rigaut, S.; Roussel, C.; Autschbach, J.; Crassous, J.; Réau, R. *J. Am. Chem. Soc.* **2012**, *134*, 15628−15631.
(8) Biet, T.; Fihey, A.; Cauchy, T.; Vanthuyne, N.; Roussel, C.; Crassous, J.; Avarvari, N. *Chem.—Eur. J.* **2013**, *19*, 13160−13167.
(9) Zak, J. K.; Miyasaka, M.; Rajca, S.; Lapkowski, M.; Rajca, A. *J. Am. Chem. Soc.* **2010**, *132*, 3246−3247.
(10) (a) Pospíšil, L.; Teplý, F.; Gál, M.; Adriaenssens, L.; Horáček, M.; Severa, L. *Phys. Chem. Chem. Phys.* **2010**, *12*, 1550−1556. (b) Pospíšil, L.; Bednárová, L.; Štěpánek, P.; Slavíček, P.; Vávra, J.; Hromadová, M.; Dlouhá, H.; Tarábek, J.; Teplý, F. *J. Am. Chem. Soc.* **2014**, *136*, 10826−10829.
(11) (a) Pochorovski, I.; Boudon, C.; Gisselbrecht, J.-P.; Ebert, M.-O.; Schweizer, W. B.; Diederich, F. *Angew. Chem., Int. Ed.* **2012**, *51*, 262−266. (b) Pochorovski, I.; Ebert, M.-O.; Gisselbrecht, J.-P.; Boudon, C.; Schweizer, W. B.; Diederich, F. *J. Am. Chem. Soc.* **2012**, *134*, 14702−14705. (c) Pochorovski, I.; Milić, J.; Kolarski, D.; Gropp, C.; Schweizer, W. B.; Diederich, F. *J. Am. Chem. Soc.* **2014**, *136*, 3852−3858.
(12) (a) Yang, B.; Liu, L.; Katz, T. J.; Liberko, C. A.; Miller, L. L. *J. Am. Chem. Soc.* **1991**, *113*, 8993−8994. (b) Liberko, C. A.; Miller, L. L.; Katz, T. J.; Liu, L. *J. Am. Chem. Soc.* **1993**, *115*, 2478−2482.
(13) (a) Nuckolls, C.; Katz, T. J.; Castellanos, L. *J. Am. Chem. Soc.* **1996**, *118*, 3767−3768. (b) Verbiest, T.; Van Elshocht, S.; Kauranen, M.; Hellemans, L.; Snauwaert, J.; Nuckolls, C.; Katz, T. J.; Persoons, A. *Science* **1998**, *282*, 913−915. (c) Katz, T. J. *Angew. Chem., Int. Ed.* **2000**, *39*, 1921−1923.
(14) Only one example of a highly substituted helicene *o*-bisquinone was reported so far. Dreher, S. D.; Paruch, K.; Katz, T. J. *J. Org. Chem.* **2000**, *65*, 806−814.
(15) (a) Zanello, P.; Corsini, M. *Coord. Chem. Rev.* **2006**, *250*, 2000−2022. (b) Kaim, W.; Schwederski, B. *Coord. Chem. Rev.* **2010**, *254*, 1580−1588.
(16) (a) Barltrop, J. A.; Jeffreys, J. A. D. *J. Chem. Soc.* **1954**, 154−159. (b) Miao, S.; Brombosz, S. M.; Schleyer, P. v. R.; Wu, J. I.; Barlow, S.; Marder, S. R.; Hardcastle, K. I.; Bunz, U. H. F. *J. Am. Chem. Soc.* **2008**, *130*, 7339−7344.
(17) (a) Grimme, S.; Harren, J.; Sobanski, A.; Vögtle, F. *Eur. J. Org. Chem.* **1998**, 1491−1509. (b) Furche, F.; Ahlrichs, R.; Wachsmann, C.; Weber, E.; Sobanski, A.; Vögtle, F.; Grimme, S. *J. Am. Chem. Soc.* **2000**, *122*, 1717−1724. (c) Rulíšek, L.; Exner, O.; Cwiklik, L.; Jungwirth, P.; Starý, I.; Pospíšil, L.; Havlas, Z. *J. Phys. Chem. C* **2007**, *111*, 14948−14955. (d) Nakai, Y.; Mori, T.; Inoue, Y. *J. Phys. Chem. A* **2013**, *117*, 83−93.
(18) (a) Reetz, M. T.; Beuttenmüller, E. W.; Goddard, R. *Tetrahedron Lett.* **1997**, *38*, 3211−3214. (b) Reetz, M. T.; Sostmann, S. *J. Organomet. Chem.* **2000**, *603*, 105−109. (c) Dreher, S. D.; Katz, T. J.; Lam, K.-C.; Rheingold, A. L. *J. Org. Chem.* **2000**, *65*, 815−822. (d) Sato, I.; Yamashima, R.; Kadowaki, K.; Yamamoto, J.; Shibata, T.; Soai, K. *Angew. Chem., Int. Ed.* **2001**, *40*, 1096−1098. (e) Takenaka, N.; Sarangthem, R. S.; Captain, B. *Angew. Chem., Int. Ed.* **2008**, *47*, 9708−9710. (f) Takenaka, N.; Chen, J.; Captain, B.; Sarangthem, R. S.; Chandrakumar, A. *J. Am. Chem. Soc.* **2010**, *132*, 4536−4537. (g) Peng, Z.; Takenaka, N. *Chem. Rec.* **2012**, *13*, 28−42. (h) Yavari, K.; Aillard, P.; Zhang, Y.; Nuter, F.; Retailleau, P.; Voituriez, A.; Marinetti, A. *Angew. Chem., Int. Ed.* **2014**, *53*, 861−865.
(19) (a) Nakazaki, M.; Yamamoto, K.; Ikeda, T.; Kitsuki, T.; Okamoto, Y. *J. Chem. Soc., Chem. Commun.* **1983**, 787−788. (b) Deshayes, K.; Broene, R. D.; Chao, I.; Knobler, C. B.; Diederich, F. *J. Org. Chem.* **1991**, *56*, 6787−6795. (c) Owens, L.; Thilgen, C.; Diederich, F.; Knobler, C. B. *Helv. Chim. Acta* **1993**, *76*, 2757−2774. (d) Weix, D. J.; Dreher, S. D.; Katz, T. J. *J. Am. Chem. Soc.* **2000**, *122*, 10027−10032. (e) Reetz, M. T.; Sostmann, S. *Tetrahedron* **2001**, *57*, 2515−2520. (f) Anger, E.; Iida, H.; Yamaguchi, T.; Hayashi, K.; Kumano, D.; Crassous, J.; Vanthuyne, N.; Roussel, C.; Yashima, E. *Polym. Chem.* **2014**, *5*, 4909−4914.
(20) (a) Ernst, K.-H.; Neuber, M.; Grunze, M.; Ellerbeck, U. *J. Am. Chem. Soc.* **2001**, *123*, 493−495. (b) Fasel, R.; Parschau, M.; Ernst, K.-H. *Angew. Chem., Int. Ed.* **2003**, *42*, 5178−5181. (c) Fasel, R.; Parschau, M.; Ernst, K.-H. *Nature* **2006**, *439*, 449−452. (d) Stöhr, M.; Boz, S.; Schär, M.; Nguyen, M.-T.; Pignedoli, C. A.; Passerone, D.; Schweizer, W. B.; Thilgen, C.; Jung, T. A.; Diederich, F. *Angew. Chem., Int. Ed.* **2011**, *50*, 9982−9986. (e) Shchyrba, A.; Nguyen, M.-T.; Wäckerlin, C.; Martens, S.; Nowakowska, S.; Ivas, T.; Roose, J.; Nijs, T.; Boz, S.; Schär, M.; Stöhr, M.; Pignedoli, C. A.; Thilgen, C.; Diederich, F.; Passerone, D.; Jung, T. A. *J. Am. Chem. Soc.* **2013**, *135*, 15270−15273.
(21) (a) Zhang, X. X.; Bradshaw, J. S.; Izatt, R. M. *Chem. Rev.* **1997**, *97*, 3313−3361. (b) Pu, L. *Chem. Rev.* **2004**, *104*, 1687−1716. (c) Hembury, G. A.; Borovkov, V. V.; Inoue, Y. *Chem. Rev.* **2008**, *108*, 1−73.
(22) (a) Stegmann, H. B.; Wendel, H.; Dao-Ba, H.; Schuler, P.; Scheffer, K. *Angew. Chem., Int. Ed.* **1986**, *25*, 1007−1008. (b) Stegmann, H. B.; Schaber, F.-M.; Schuler, P.; Scheffler, K. *Magn. Reson. Chem.* **1989**, *27*, 887−891. (c) Mäurer, M.; Scheffler, K.; Stegmann, H. B.; Mannschreck, A. *Angew. Chem., Int. Ed.* **1991**, *30*, 602−604. (d) Stegmann, H. B.; Mäurer, M.; Höfler, U.; Scheffler, K.; Hewgill, F. *Chirality* **1993**, *5*, 282−287. (e) Schuler, P.; Schaber, F.-M.; Stegmann, H. B.; Janzen, E. *Magn. Reson. Chem.* **1999**, *37*, 805−813.
(23) Vollhardt, K. P. C. *Angew. Chem., Int. Ed.* **1984**, *23*, 539−556.
(24) (a) Stará, I. G.; Starý, I.; Kollárovič, A.; Teplý, F.; Šaman, D.; Tichý, M. *J. Org. Chem.* **1998**, *63*, 4046−4050. (b) Teplý, F.; Stará, I. G.; Starý, I.; Kollárovič, A.; Šaman, D.; Rulíšek, L.; Fiedler, P. *J. Am. Chem. Soc.* **2002**, *124*, 9175−9180. (c) Míšek, J.; Teplý, F.; Stará, I. G.; Tichý, M.; Šaman, D.; Císařová, I.; Vojtíšek, P.; Starý, I. *Angew. Chem., Int. Ed.* **2008**, *47*, 3188−3191. (d) Jančařík, A.; Rybáček, J.; Cocq, K.; Vacek Chocholoušová, J.; Vacek, J.; Pohl, R.; Bednárová, L.; Fiedler, P.; Císařová, I.; Stará, I. G.; Starý, I. *Angew. Chem., Int. Ed.* **2013**, *52*, 9970−9975. (e) Vacek Chocholoušová, J.; Vacek, J.; Andronova, A.; Míšek, J.; Songis, O.; Šámal, M.; Stará, I. G.; Meyer, M.; Bourdillon, M.; Pospíšil, L.; Starý, I. *Chem.—Eur. J.* **2014**, *20*, 877−893.
(25) Brown, S. N. *Inorg. Chem.* **2012**, *51*, 1251−1260.
(26) Ueda, A.; Ogasawara, K.; Nishida, S.; Ise, T.; Yoshino, T.; Nakazawa, S.; Sato, K.; Takui, T.; Nakasuji, K.; Morita, Y. *Angew. Chem., Int. Ed.* **2010**, *49*, 6333−6337.
(27) Krejčik, M.; Daněk, M.; Hartl, F. *J. Electroanal. Chem.* **1991**, *317*, 179−187.
(28) Frisch, M. J.; Trucks, G. W.; Schlegel, H. B.; Scuseria, G. E.; Robb, M. A.; Cheeseman, J. R.; Scalmani, G.; Barone, V.; Mennucci, B.; Petersson, G. A.; Nakatsuji, H.; Caricato, M.; Li, X.; Hratchian, H. P.; Izmaylov, A. F.; Bloino, J.; Zheng, G.; Sonnenberg, J. L.; Hada, M.; Ehara, M.; Toyota, K.; Fukuda, R.; Hasegawa, J.; Ishida, M.; Nakajima, T.; Honda, Y.; Kitao, O.; Nakai, H.; Vreven, T.; Montgomery, J. A., Jr.; Peralta, J. E.; Ogliaro, F.; Bearpark, M.; Heyd, J. J.; Brothers, E.; Kudin, K. N.; Staroverov, V. N.; Kobayshi, R.; Normand, J.; Raghavachari, K.; Rendell, A.; Burant, J. C.; Iyengar, S. S.; Tomasi, J.; Cossi, M.; Rega, N.; Millam, J. M.; Klene, M.; Knox, J. E.; Cross, J. B.; Bakken, V.; Adamo, C.; Jaramillo, J.; Gomperts, R.; Stratmann, R. E.; Yazyev, O.; Austin, A. J.; Cammi, R.; Pomelli, C.; Ochterski, J. W.; Martin, R. L.; Morokuma, K.; Zakrzewski, V. G.; Voth, G. A.; Salvador, P.; Dannenberg, J. J.; Dapprich, S.; Daniels, A. D.; Farkas, Ö.; Foresman, J. B.; Ortiz, J. V.; Cioslowski, J.; Fox, D. J. *Gaussian 09*, revision A.1; Gaussian, Inc.: Wallingford, CT, 2009.
(29) For a study on a neutral [4]helicene-based radical see the following: Ueda, A.; Wasa, H.; Suzuki, S.; Okada, K.; Sato, K.; Takui, T.; Morita, Y. *Angew. Chem., Int. Ed.* **2012**, *51*, 6691−6695.
(30) (a) Szwarc, M. *Acc. Chem. Res.* **1969**, *2*, 87−96. (b) Lee, L.; Adams, R.; Jagur-Grodzinski, J.; Szwarc, M. *J. Am. Chem. Soc.* **1971**, *93*, 4149−4154.
(31) Bock, H.; Jaculi, D. *Angew. Chem., Int. Ed.* **1984**, *1984*, 305−307.
(32) Weil, J. A.; Bolton, J. R. *Electron Paramagnetic Resonance*; 2nd ed.; John Wiley & Sons, Inc.: Hoboken, NJ, 2007.
(33) Seebach, D. *Angew. Chem., Int. Ed.* **1988**, *27*, 1624−1654.

(34) Burk, P.; Koppel, I. A.; Koppel, I.; Kurg, R.; Gal, J.-F.; Maria, P.-C.; Herreros, M.; Notario, R.; Abboud, J.-L. M.; Anvia, F.; Taft, R. W. *J. Phys. Chem. A* **2000**, *104*, 2824−2833.
(35) (a) Benaglia, M.; Rossi, S. *Org. Biomol. Chem.* **2010**, *8*, 3824−3830. (b) Kotani, S.; Sugiura, M.; Nakajima, M. *Chem. Rec.* **2013**, *13*, 362−370.
(36) (a) Fallis, I. A.; Murphy, D. M.; Willock, D. J.; Tucker, R. J.; Farley, R. D.; Jenkins, R.; Strevens, R. R. *J. Am. Chem. Soc.* **2004**, *126*, 15660−15661. (b) Murphy, D. M.; Fallis, I. A.; Willock, D. J.; Landon, J.; Carter, E.; Vinck, E. *Angew. Chem., Int. Ed.* **2008**, *47*, 1414−1416.
(37) Murphy, D. M.; Caretti, I.; Carter, E.; Fallis, I. A.; Göbel, M. C.; Landon, J.; Van Doorslaer, S.; Willock, D. J. *Inorg. Chem.* **2011**, *50*, 6944−6955.
(38) Mortimer, R. J.; Dyer, A. L.; Reynolds, J. R. *Displays* **2006**, *27*, 2−18.
(39) (a) Scholz, M.; Gescheidt, G. *J. Chem. Soc., Chem. Commun.* **1994**, 239−240. (b) Scholz, M.; Gescheidt, G.; Daub, J. *J. Chem. Soc., Chem. Commun.* **1995**, 803−804. (c) Barbosa, F.; Péron, V.; Gescheidt, G.; Fürstner, A. *J. Org. Chem.* **1998**, *63*, 8806−8814. (d) Exner, K.; Cullmann, O.; Vögtle, M.; Prinzbach, H.; Grossmann, B.; Heinze, J.; Liesum, L.; Bachmann, R.; Schweiger, A.; Gescheidt, G. *J. Am. Chem. Soc.* **2000**, *122*, 10650−10660.
(40) Mahlau, M.; List, B. *Angew. Chem., Int. Ed.* **2013**, *52*, 518−533.